# Energy Consumption in Multi-BD Symbiotic Radio System assisted 6G Network: A QoS Constraint Approach

Rahman Saadat Yeganeh [1], Mohammad Javad Omidi [1] and

Mohammad Ghavami [2], *Senior Member, IEEE*

## Abstract

Symbiotic radio (SR) is a novel paradigm in cognitive ambient backscatter communication, which makes the connection of devices without the need to reallocation of the frequency spectrum and complex energy infrastructure and so, can turn a 6G network into a green communication. In the system model of this paper, the base stations (BSs) with the active antennas, symbiotic backscatter devices (SBDs) and symbiotic user equipment (SUE) are considered. The main purpose is to minimize the energy consumption (EC) in the SR network and increase energy efficiency (EE) by taking into account to fulfillment of the minimum required throughput for SBDs. To this end, we introduce a new scheduling system called Timing SR (T-SR) to optimal resource allocation between SBDs. In this system, SBDs harvest energy from ambient signals and then send their information without interfering with each other, even in simultaneous transmission, to SUE by using the carrier of its signal. The main optimization problem has non-convex objective functions and constraints. To solve it, we use the novel mathematical methods called conic quadratic representation (CQR) and sequential quadratic (SQ) techniques. Finally, simulation results demonstrate the superiority of the proposed method compared to other outlined schemes in reducing the EC.

## Index Terms

Symbiotic radio, backscatter communication, 6G, energy efficiency, IoT, optimal resource allocation.

[1]Department of Electrical and Computer Engineering, Isfahan University of Technology, Isfahan, IR 8415683111

[2]Electrical and Electronic Engineering Department, London South Bank University, London SE1 0AA, U.K.

# I. INTRODUCTION

## A. Background

With the exponential increase of the internet-of-things (IoT) and wireless devices in the future wireless networks and the required massive connectivity, energy consumption (EC) will increase dramatically. That is a big challenge for future networks [1] and is one of the most crucial requirements for the design and implementation of IoT networks [2]. Generally, cellular and IoT devices are usually powered by batteries or other embedded energy sources [3], [4] and this is contrary to the requirements of the internet of everything (IoE) in beyond 5G (B5G) and 6G networks [5]. Also, it is not practical to replace/recharge the batteries regularly, especially in harsh environments like toxic nuclear areas [6], large-scale network systems, and building-embedded applications [7]. To implement the infrastructure of future networks, and achieve sustainable and green IoT, it is essential to build a self-sustaining system to reduce maintenance costs [8]–[11]. The best way to achieve the above goals is to use wireless energy harvesting [12], [13]. By using the wireless energy harvesting technologies from ambient signals, the energy efficiency of the network will be significantly improved [14]–[16].

Wireless energy harvesting benefits from active and passive technologies developed for telecommunication systems and networks, such as wireless powered communication networks (WPCN) [17], simultaneous wireless information and power transfer (SWIPT) [18], reconfigurable intelligent surface (RIS), bistatic and ambient backscatter communication (AmBC) [19] and SR [20]. Moreover, AmBC, cognitive radio (CR) and SR can also be used for spectrum sharing [21].

CR technology has been considered to enhance spectrum efficiency in IoT networks [22]. In this system, the secondary user is allowed to access the spectrum allocated to the primary user in an opportunistic or spectrum sharing manner, which makes it challenging to increase the spectrum efficiency [23], [24]. On the other hand, user equipment in the CR system uses the power-consuming active components, which leads to reduced device battery life, and limits the development of emerging services in future wireless networks [25].

In recent years, AmBC has been used to design transceivers without requiring active components, thus the power consumption can be greatly reduced. It can make battery-free communications with enhanced energy efficiency. Also, AmBC enables backscatter devices (BDs) to modulate their information over the ambient RF signals (such as Cellular, TV, or WiFi signals); therefore, there is no need for complex processes to reallocate frequency (which is very limited)

to BDs; hence, spectral efficiency is greatly increased [19], [26].

There are some disadvantages to AmBC since ambient RF sources are dynamic, and thus the performance of an AmBC may not be stable. Also, since the transmission power and position of ambient RF sources are not controllable, the deployment of an AmBC to achieve optimal performance is more complex. On the other hand, AmBC and BS signals may interfere with the receiver as they both send signals at the same operating frequency [27].

In a 6G network, the low energy consumption, extended battery charge length and increased efficiency of the allocated frequency band are three important research areas [28], [29]. The main purpose of 6G communications is to make the devices battery-free whenever and wherever possible [30].

In this paper, a new technique called symbiotic radio (SR) system with a resource scheduling system called timing-SR or T-SR is proposed to use the benefits and overcome the drawbacks of AmBC and CR as a promising solution to green IoT networks. It can enhance spectrum efficiency by using mutualism sharing the spectrum and also can increase energy efficiency by using the passive components [31]–[34]. In the SR system, passive IoT devices harvest the energy from ambient signals wirelessly, in the cellular or cell-free networks and establish stable communications [35], [36]. Moreover, the transmitter and receiver communicate with each other in a coexistence manner; hence, the SR can support massive wireless connections in dense networks [22], [25];

*B. Related Works*

Energy efficiency (EE), as an objective, is brought up in many types of research. In [37], authors consider a basic SR model which consists of three nodes BS, BD, and UE. The BS beamform its signal to establish joint primary and BD transmissions, while the UE can decode the signals from both BS and the BD.

In [38], authors tried to reach the maximum EE with efficient resource allocation among BD with considering the guarantee of the quality of service (QoS) for users in NOMA-backscatter communication (BC) networks. To overcome the drawbacks of the BC systems, the SR system has been considered in paper [39]. In this paper, the authors consider the EE maximization problem of SR system with multiple BDs, which enables to harvesting of energy from the ambient signal. In the Scheduling system, the time division multiple access (TDMA) protocol is

used and BDs take turns modulating their information on the ambient signal and sending their information to the receiver.

The symbiotic communication model with multiple passive BDs was proposed in [40]. For this purpose, passive users use mutually coding and decoding algorithms to achieve orthogonal chips with different chip lengths and chip transmission rates. Hence, the interference-free transmission between multiple user signals is realized, and users can send their information concurrently. Also, in [41], the authors consider a multi-BD SR system in which a cooperative receiver can receive and detect the collected data from the PT and the multiple BDs, simultaneously. For this purpose, they assume a random code-assisted multiple access scheme for the multi-BD, with which the transmit power of the BS and the reflection coefficients of the BDs are jointly optimized. In this scheme, each BD chooses its random code to backscatter its information instantaneously.

*C. Contribution*

The number of IoT devices and data rates for transmitting information in future heterogeneous networks is increasing rapidly [42]. Therefore, there is a need to use new frequency spectrums and also the EC of these networks will increase sharply. As mentioned in the previous section, EE is gradually accepted as an important design criterion for future networks [43], because proper EE has several benefits including reducing greenhouse gas emissions [44], reducing demand for energy imports, and reducing the complex implementation of networks and improving the economy [45]. In accordance, we study a novel cognitive backscattering system based on wireless power transfer in a passive system to enhance EE of dense networks such as cellular or cell-free communication and IoT networks. In this paper, we use SR system technology to prevent interference between IoT devices and ambient transmitters, as well as to eliminate the need for IoT devices to reallocate spectrum and use ambient energy signals to extend the life of these devices. In the system model of this paper, we try to minimize the network EC by guaranteeing a minimum required throughput for multiple IoT devices (SBDs) that were randomly distributed in this network.

The major contributions of this paper are summarized as follows:

- First, we present a general system model for the proposed SR system and investigate that when SBDs have information to send, they can send it to their intended destination without interfering with each other and BSs. In this model, a QoS constraint is considered to guarantee the minimum transmission rate of SBDs.

- In timing resources allocation, the T-SR mode has been introduced for the SBDs in the SR network. In T-SR mode we consider a 2-mode variable time slot consisting of EHS and DTI. In this strategy, users can always harvest energy as much as needed to transmit their information. This strategy helps to reduce EC in the network because SBDs do not have idle mode and can send their information in continuous time slots.

- The general proposed model is formulated by a non-convex optimization problem with an objective function to minimize EC in the network subject to the required SBDs throughput and amount of energy harvesting. The non-convex optimization problem is reformulated and solved by two novel mathematical techniques referred to sequential quadratic (SQ) and conic quadratic representation (CQR).

- The power consumption in the proposed SR system with the T-SR scheduling mode is compared with the TDMA mode. Also, the SR system is suitable for dense networks such as IoT and 6G networks, is compared with other well-known IoT protocols.

The remainder of this paper is organized as follows. Section II introduces the proposed system model for the SR. In Section III, we investigate the EC problem by considering the minimum user throughput requirement. Moreover, in this section SQ and CQR methods are introduced and the main problem is solved by using them. In Section IV, the computational complexity of the proposed methods is analyzed. In section V, a general comparison between the SR system and other popular IoT protocols is provided. In the VI section, to confirm our analytical findings, the results of the simulations and comparisons with other work are performed, finally, the conclusions and future work are given in section VII.

Notations: $\langle a, b \rangle$ denotes the inner product of $a$ and $b$, $Tr\left(\mathbf{A}\right)$, $\mathbf{A}^H$, $\mathbf{A}^T$, $\|\mathbf{A}\|$ denote the trace, conjugate transpose, transpose, and norm of the matrix $\mathbf{A}$, respectively. The positive semi-definite was denoted as $\mathbf{A} \succeq 0$ and $\nabla$ shows the gradient operator.

## II. SYSTEM MODEL

As illustrated in the system model of Fig.1 a symbiotic radio system with $N_a$ active base stations (BSs) equipped with $N_s$ massive MIMO antennas to send directive signals in the network, one symbiotic user equipment (SUE) with a single antenna and I single antenna symbiotic backscatter devices (SBDs) are considered. The SBDs are randomly distributed and harvest energy from the signal transmitted by BSs. In the proposed system model, symbiotic radio
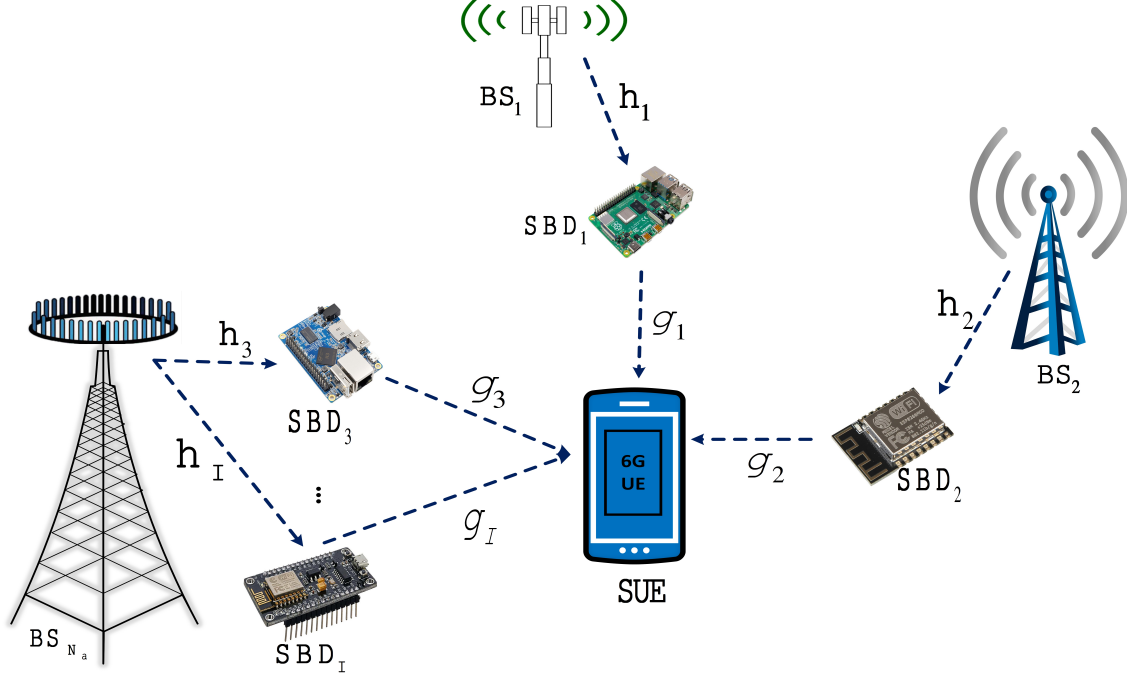
Fig. 1: Symbiotic radio system model with multiple SBDs

(SR) communication is considered to have two main operating phases. In the first phase, SBDs receive a signal from BSs, and harvest as much energy as needed from the received signal. In this phase, SBDs, as IoT devices, constantly sense the environment; hence, this phase is called energy harvesting and environment sensing (EHS). In the second phase, SBDs decode and remove the information from the BS signal to obtain the carrier frequency, and send their data to SUE over this carrier. Therefore, this phase is called decoding the ambient signal and transmitting information (DTI) by SBDs. In all situations, it is assumed that channel state information (CSI) is fully available. SUEs may also receive the signal from the BSs through the direct link in addition to the SBDs' signal. We assume that the signal received from the direct link is well eliminated by various techniques such as beamforming, non-orthogonal multiple access (NOMA), and successive interference-cancellation (SIC) [26], [46], [47]; hence, only the backscattered signal can be considered in SUE.

As shown in Fig.1, SBDs can use the carrier frequency of the received ambient signal from the nearest BS. In this case, based on the frequency division multiple access (FDMA) method, and due to the coexistence of devices, the separation of SBDs information is well carried out in SUE [48]. Otherwise, if several SBDs are covered by one BS, they may use the same carrier

frequency to send their information simultaneously. In this situation, SBDs and SUE should use mutually coding and decoding algorithms to achieve orthogonal chips with different chip lengths and chip transmission rates. Hence, the interference-free transmission between multiple user signals is realized, thereby achieving multi-user symbiosis [40], [41].

According to the above description, in the SR system, since SUE and SBDs exchange information in a collaborative method, and the SUE has information about the signal characteristics sent by the SBDs, it can separate the information of SBDs correctly, and thus, interference of the SBDs information is reduced in SUE and can be ignored [25], [49]. For this reason, it is assumed that in the SR system, all IoT devices (SBDs) can send their information without interference at all times.

The SBDs receive the ambient signal from BSs in $\tau_j, j = 1, 2, ..., J$ time slots. In this timing system, $J$ is the total number of time slots allocated to SBDs on the network, which is assumed to be equal to $I$. In the SR system, the time slots are identical and SBDs are allowed to use one or more time slots in a one-time frame. The number of time slots required to send information is proportional to the length of information in each SBD and the energy required to send this information. In Fig.2, the scheduling of energy harvesting by SBDs and data transmission from SBDs to SUEs is shown. In the SR system, we define this time division duplexing (TDD) as timing-SR (T-SR) mode. In each time frame with the length of T, SBDs start data transmission at the beginning of a time slot and finish at the end of that or another time slot. The number of time slots used depends on the volume of data. We define $\upsilon$ as the set of indexes for all time slots used for data transmission. For example, in Fig.2 the data is transmitted by $\mathrm{SBD}_2$ in $\tau_2$, $\tau_3$ and $\tau_4$ time slots so $\upsilon = \{2, 3, 4\}$. Therefore, in T-SR mode:

$$
\tau_{j=1,2,...,J} = \left\{
\begin{array}{ll}
\mathrm{DTI} & j \in \upsilon \\
\mathrm{EHS} & j \notin \upsilon
\end{array}
\right.
\tag{1}
$$

It is considered that all SBDs have the required initial charge. Since SBDs has only a single antenna, so, they can only either harvest energy or decode and transmit signal at a time, so during the transmission of SBDs' data, whenever their battery charge is finished, they switch from DTI mode to EHS mode and start recharging by ambient signals.

The T-SR mode in the SR network is used to increase EE and throughput; moreover, there is no need to perform complex processing on the network core to allocate frequency to SBD devices, as they use ambient signal frequencies. In this paper, we will study the EC of the SR
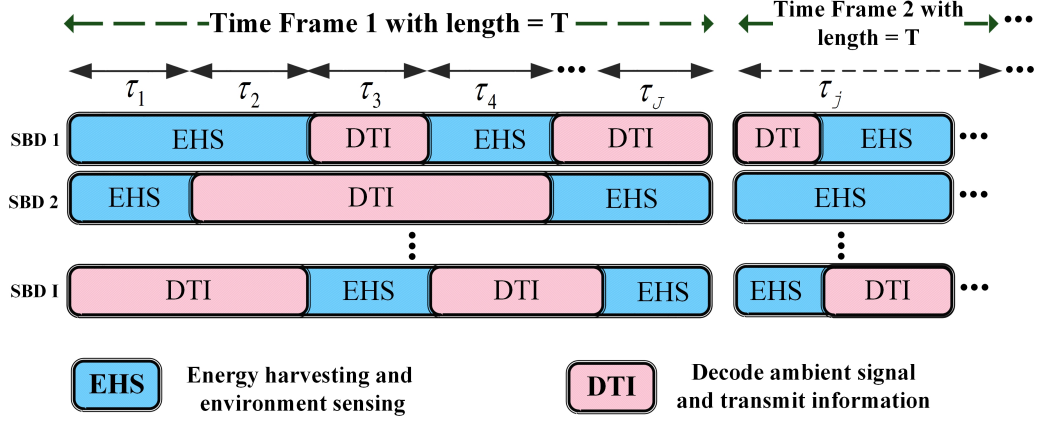
Fig. 2: The TDD transmission frame for EHS and DTI modes in T- SR instantaneous transmission information mode

system and will compare EC in the SR scheduling method (T-SR) with the TDMA scheme in the simulation section.

## A. Problem Formulation

In Fig.1, we assume that the N is the sum of all antennas in all BSs ($N = N_a \times N_s$). The signal transmitted by n-th antenna on BSs to all SBDs in j-th time slot is denoted by $x_{n,j}$ with zero mean and $E\left[|x_{n,j}|^2\right] = p_n$ which is the transmit power of n-th antenna. In this paper, $p_n$ is considered in $x_{n,j}$ and it is not shown in relations. The signal vector at the time slot $\tau_j$ is defined as $\mathbf{x}_j \triangleq [x_{1,j}, x_{2,j}, ..., x_{N,j}]^T$ and The channel vector from n-th antenna on BSs to SBD$_i$ is modeled by $h_{n,i}$. Also, we define the complex channel vector to SBD$_i$ as $\mathbf{h}_i \triangleq [h_{1,i}, h_{2,i}, ..., h_{N,i}]^T$ which is flat fading and constant during a one-time frame. Therefore, the received signal in the SBD$_i$ at the time slot $\tau_j$ is:

$$y_{i,j} = \mathbf{h}_i^H \mathbf{x}_j + n_i ; \quad i, j \in \boldsymbol{\Psi} \tag{2}$$

where $\boldsymbol{\Psi} \triangleq [1, 2, ..., I]$ and $n_i \sim CN(0, \sigma_i^2)$ is the circularly symmetric complex Gaussian (CSCG) noise and it is assumed to be independent of the signal $\mathbf{x}_j$. According to Eq.(2), the maximum energy harvested by the SBD$_i$ in the $\tau_j$ is:

$$\varepsilon_{ij} = \eta_i \tau_{j \notin \upsilon} E\left[|y_{i,j}|^2\right] = \eta_i \tau_{j \notin \upsilon} \mathbf{x}_j^H \mathbf{h}_i \mathbf{h}_i^H \mathbf{x}_j , \quad i, j \in \boldsymbol{\Psi} \tag{3}$$

where $0 \leq \eta_i \leq 1$ is the efficiency of energy harvesting or reflection coefficient by SBD$_i$

The total energy sent by all BSs is the sum of the energy sent by each of them ( $E_T$ ), so:

$$E_T = \sum_{n=1}^{N} E_{T_{BS}}^n \tag{4}$$

$\mathbf{E_T}$ can also be expressed as the sum of the energy of transmitted signals by all BSs at all times during a frame.

$$E_T = \sum_{j=1}^{J} \tau_j \mathbf{x}_j^H \mathbf{x}_j \tag{5}$$

The main purpose of this paper is to minimize $E_T$ to increase EE in the SR system while satisfying the minimum required data rate of the SBDs. In the SR networks, passive modules are used and special electronic circuits with very low power consumption are employed; therefore all power consumptions other than radiation power, i.e. circuit power consumption for hardware processing is ignored in our model. In a real-world urban environment, SBDs may be covered by multiple BSs and can harvest energy from all ambient signals, faster than harvesting energy from one broadcasting antenna.

It is necessary to mention that since SBDs have a passive antenna, they receive little noise, which can be ignored [41], [50]; hence these devices can remove the noise $n_i$ in the $y_{i,j}$ when decoding data. Also, to send SBDs signal information, we assume that the SNR of the received ambient signal in the SBDs is acceptable and therefore, they can correctly decode and delete the information in the received signal from the BSs. Hence, instead of the signal $\mathbf{h}_i^H \mathbf{x}_j \mathbf{s}_i$ , the signal $\mathbf{s_i}$ is sent by the SBDs. Where $\mathbf{s_i} \triangleq [s_{i,a}, s_{i,b}, ..., s_{i,z}]_{\{a,b,...,z\} \in \upsilon}^T$ is the normalized modulated information signal transmitted from $\mathrm{SBD_i}$ to the SUE in all time slots of the DTI set ( $\upsilon$ ).

Following the above description after removing the noise and deleting the information on the carrier of the received signal at the SBDs the information of each SBD ($\boldsymbol{s_i}$), is placed on that carrier and sent to the desired destination (SUE). Therefore, the received signal at SUE, transmitted by the $\mathrm{SBD_i}$ in the time slot $\tau_{j \in \upsilon}$ is:

$$y_{i,j \in \upsilon}^{UE} = \sqrt{p_i} g_i s_{i,j \in \upsilon} + n_{UE} \tag{6}$$

where $g_i$ is the complex channel gain from $\mathrm{SBD_i}$ to SUE and $p_i$ is the power of $\mathrm{SBD_i}$ to transmit the signals and $n_{UE} \sim CN(0, \sigma_{UE}^2)$ is the CSCG noise at the SUE. According to Eq.(6) the SNR for decoding $s_{i,j \in \upsilon}$ in the SUE is:

$$\mathrm{SNR}_i^{UE} = \frac{p_i |g_i|^2}{\sigma_{UE}^2} \tag{7}$$

Since in the SR network, the passive IoT devices are used and these devices do not have active components to consume energy; therefore, it can be considered that each SBD uses all amount of harvested energy to send their signals, then the relation $p_i\tau_{j\in\upsilon} = \sum_{j=1,j\notin\upsilon}^{J} \varepsilon_{ij}$ is established and Eq.(7) can be rewritten as follows:

$$\text{SNR}_i^{UE} = \frac{|g_i|^2 \sum_{j=1,j\notin\upsilon}^{J} \varepsilon_{ij}}{\tau_{j\in\upsilon}\sigma_{UE}^2} \tag{8}$$

## III. ENERGY AND RATE OPTIMIZATION

In this section, an optimization problem is proposed. We aim to minimize the sum of the transmit energy by all BSs by jointly optimizing the transmit energy and information signal, time scheduling, and energy harvesting by SBDs. Also, the energy of the signal transmitted by BSs must satisfy the minimum specified SBDs information rate, defined as $C_i$. To ensure that each of the SBDs can send their information to the destination (SUE) in the minimum throughput $C_i$, we use the Shannon channel capacity relation to specify the minimum capacity for the channel between them and consider the constraint for all SBDs. So, the instantaneous achievable rate (bps/Hz) of the $SBD_i$ is:

$$R_i = \tau_{j\in\upsilon}\log_2\left(1 + \frac{|g_i|^2 \sum_{j=1,j\notin\upsilon}^{J} \varepsilon_{ij}}{\tau_{j\in\upsilon}\sigma_{UE}^2}\right) \geq C_i \tag{9}$$

According to the above description and Eq.(3) and Eq.(9), the general optimization problem for the mentioned objectives and constraints is defined as follows:

$$\min_{\mathbf{x}_j,\tau_j,\varepsilon_{ij}} \quad \text{E}_\text{T} = \sum_{j=1}^{J}\tau_j\mathbf{x}_j^H\mathbf{x}_j \tag{10}$$

$$\text{s.t.} \quad R_i \geq C_i \qquad\qquad i \in \boldsymbol{\Psi} \tag{10a}$$

$$\tau_j \geq 0 \qquad\qquad j \in \boldsymbol{\Psi} \tag{10b}$$

$$\sum_{j=1}^{J}\tau_j \leq T \qquad\qquad j \in \boldsymbol{\Psi} \tag{10c}$$

$$\varepsilon_{ij} \leq \eta_i\tau_{j\notin\upsilon}\mathbf{x}_j^H\mathbf{h}_i\mathbf{h}_i^H\mathbf{x}_j \qquad i,j \in \boldsymbol{\Psi} \tag{10d}$$

The problem expressed in Eq.(10) is non-convex due to objective function and constraint (10d). However, constraint (a) is convex since it can be seen as a composition of perspective

of $\log\left(1+\alpha x\right), a > 0$ and an affine function of $x = \varepsilon_{ij}$ . To overcome the non-convexity of objective function, an auxiliary variable $\gamma_j = \mathbf{x}_j^H \mathbf{x}_j$ is defined and as a result, another non-convex constraint appears. It can be relaxed by adding the following convex constraint:

$$\gamma_j \geq \mathbf{x}_j^H \mathbf{x}_j \quad , j \in \mathbf{\Psi} \tag{11}$$

So, the new problem is:

$$\min_{\mathbf{x}_j, \tau_j, \gamma_j, \varepsilon_{ij}} \mathrm{E_T} = \sum_{j=1}^{J} \tau_j \gamma_j \tag{12}$$

$$\text{s.t} \quad (10a), (10b), (10c), (10d) \tag{12a}$$

$$\gamma_j \geq \mathbf{x}_j^H \mathbf{x}_j \qquad j \in \mathbf{\Psi} \tag{12b}$$

The problem (12) is still non-convex. Also, this problem contains the perspective of logarithm function which is convex but not disciplined convex. Disciplined convex problems can be solved efficiently by using the primal-dual interior point method and solver technologies progressed maturely over recent years. In the four following subsections (A, B, C, D), the non-convexity parts of the general optimization problem are investigated and the problem will become convex by various techniques.

## A. Overcoming Non-Convex Objective Function

To overcome the non-convexity of objective function we can rewrite it as follows:

$$\sum_{j=1}^{J} \tau_j \gamma_j = \frac{1}{4} \left[ \sum_{j=1}^{J} \left( \tau_j + \gamma_j \right)^2 - \sum_{j=1}^{J} \left( \tau_j - \gamma_j \right)^2 \right], j \in \mathbf{\Psi} \tag{13}$$

Eq.(13) is the difference between two convex functions. By defination $f_1 \triangleq \left( \tau_j - \gamma_j \right)^2$ , the second term $-f_1$ is a concave function and its upper bound can be calculated by a linear function. The upper bound of that relation performed by inner approximation [51] and sub-gradient method [52] around the feasible (initial) point $\left( \hat{\tau}_j, \hat{\gamma}_j \right)$ as follows:

$$\begin{aligned} f_1 &\leq \left( \hat{\tau}_j - \hat{\gamma}_j \right)^2 + \nabla_{\tau_j, \gamma_j} f_1 \left( \hat{\tau}_j, \hat{\gamma}_j \right) \left[ \left( \tau_j - \hat{\tau}_j \right), \left( \gamma_j - \hat{\gamma}_j \right) \right]^T \\ &= \left( \hat{\tau}_j - \hat{\gamma}_j \right)^2 + 2 \left( \hat{\tau}_j - \hat{\gamma}_j \right) \left[ \left( \tau_j - \hat{\tau}_j \right) - \left( \gamma_j - \hat{\gamma}_j \right) \right] \end{aligned} \tag{14}$$

Eq.(14) is replaced in the second part of Eq.(13) and in results an upper-bounded function which is a tangent line to the original function. It is shown in [51], that the upper-bounded approximation function lies quite close to the function, at least near the point of tangency which is the point placed on Eq.(13). Suppose Eq.(14) is iteratively solved and converged. Therefore, the relations (13) and (14) attain the same local optimal point.

## B. Semidefinite Relaxation of Constraint (10d)

By using the trace commutative property, we have the following equation:

$$\mathbf{x}_j^H \mathbf{h}_i \mathbf{h}_i^H \mathbf{x}_j = \mathrm{Tr}\left(\mathbf{x}_j^H \mathbf{h}_i \mathbf{h}_i^H \mathbf{x}_j\right) = \mathrm{Tr}\left(\mathbf{x}_j \mathbf{x}_j^H \mathbf{h}_i \mathbf{h}_i^H\right) \tag{15}$$

Now the constraint $(10d)$ can be reformulated by an auxiliary matrix $\mathbf{X}_j = \mathbf{x}_j \mathbf{x}_j^H$ and $\mathbf{H}_i \triangleq \mathbf{h}_i \mathbf{h}_i^H$ as follows:

$$\varepsilon_{ij} \leq \eta_i \tau_{j \notin \upsilon} Tr\left(\mathbf{X}_j \mathbf{H}_i\right) \qquad i, j \in \boldsymbol{\Psi} \tag{16}$$

So, since $\mathbf{X}_j$ is a positive semidefinite matrix, the constraint $(16)$ can be replaced by:

$$\eta_i \tau_{j \notin \upsilon} Tr\left(\mathbf{X}_j \mathbf{H}_i\right)/\varepsilon_{ij} \geq 1 \qquad i, j \in \boldsymbol{\Psi} \tag{17a}$$

$$\mathbf{X}_j \succeq 0 \qquad j \in \boldsymbol{\Psi} \tag{17b}$$

$$\mathrm{Rank}\left(\mathbf{X}_j\right) = 1 \qquad j \in \boldsymbol{\Psi} \tag{17c}$$

where the notation $\succeq$ denotes that $\mathbf{X}_j$ is a positive semidefinite. The problem is still non-convex due to the rank-one constraint given in $(17c)$. By applying the semidefinite relaxation (SDR) technique, the rank-one constraint will be dropped and the relaxed version of the main problem will be obtained [53]. The relaxed problem will be a convex semidefinite programming (SDP) problem that is solvable by interior-point methods. If the optimal solution $\mathbf{X}_j$ for the problem with the relaxed constraints (17) is rank-one, then it is also a solution for the original problem (12), which can be done by using randomization techniques [53]. In this state, we can easily extract a feasible $\mathbf{x}_j$ from $\mathbf{X}_j$.

Moreover, we know $\mathrm{Tr}(\mathbf{X}_j) \leq \lambda_{\max}(\mathbf{X}_j)$, where $f_2 \triangleq \lambda_{\max}(\mathbf{X}_j)$ denotes the maximum eigenvalue of the $\mathbf{X}_j$ and it can be rewritten as the following difference between two convex functions [54]:

$$\mathrm{Tr}\left(\mathbf{X}_j\right) - \lambda_{\max}\left(\mathbf{X}_j\right) \leq 0 \tag{18}$$

The sub-gradient of $\lambda_{\max}(\mathbf{X}_j)$ is:

$$\nabla_{\mathbf{X}_j} f_2\left(\hat{\mathbf{X}}_j\right) = \mathbf{v}_{\max}\left(\mathbf{X}_j\right) \mathbf{v}_{\max}^H\left(\mathbf{X}_j\right) \tag{19}$$

where $\mathbf{v}_{\max}\left(\mathbf{X}_j\right)$ is the maximum eigenvector corresponding to the $\lambda_{\max}(\mathbf{X}_j)$. Therefore, the lower bound of linear approximation $\lambda_{\max}(\mathbf{X}_j)$ at the point $\hat{\mathbf{X}}_j$ is as follows:

$$\begin{aligned} f_2 &\geq \lambda_{\max}\left(\hat{\mathbf{X}}_j\right) + \left\langle \nabla_{\mathbf{X}_j} f_2\left(\hat{\mathbf{X}}_j\right), \left(\mathbf{X}_j - \hat{\mathbf{X}}_j\right)\right\rangle \\ &= \lambda_{\max}\left(\hat{\mathbf{X}}_j\right) + \mathbf{v}_{\max}^H\left(\hat{\mathbf{X}}_j\right) \mathbf{v}_{\max}\left(\hat{\mathbf{X}}_j\right)\left(\mathbf{X}_j - \hat{\mathbf{X}}_j\right) \end{aligned} \tag{20}$$

By substituting Eq.(20) in the Eq.(18) the following relationship is obtained:

$$\text{Tr}\left(\mathbf{X}_j\right) \leq \mathbf{v}_{\max}^H\left(\hat{\mathbf{X}}_j\right)\mathbf{X}_j\mathbf{v}_{\max}\left(\hat{\mathbf{X}}_j\right) \tag{21}$$

Eq.(21) is defined as a convex subset of the convex set of the original equation (12) and is moved to the objective function with multiplying in coefficient $\ell$ as a penalty function [55]. The resulting problem should be solved iteratively for $\ell$ from small to large values, so as not to cause numerical instability. Herein, The constraint $(17a)$ can be represented by the difference in the convex functions method and by defining the auxiliary variable $\phi_{ij}^2 = \varepsilon_{ij}$:

$$\phi_{ij}^2 \leq \eta_i \tau_{j\notin v} Tr\left(\mathbf{X}_j \mathbf{H}_i\right) \tag{22}$$

The above inequality is equivalent to:

$$\phi_{ij}^2 + \frac{1}{4}(\eta_i Tr\left(\mathbf{X}_j \mathbf{H}_i\right) - \tau_{j\notin v})^2 \leq \frac{1}{4}(\eta_i Tr\left(\mathbf{X}_j \mathbf{H}_i\right) + \tau_{j\notin v})^2 \tag{23}$$

Since $Tr\left(\mathbf{X}_j \mathbf{H}_i\right) + \tau_{j\notin v} \geq 0$, the above CQR relation can be written in the following form:

$$\left\|\phi_{ij}, \frac{1}{2}\left(\eta_i Tr\left(\mathbf{X}_j \mathbf{H}_i\right) - \tau_{j\notin v}\right)\right\|_2 \leq \frac{1}{2}\left(\eta_i Tr\left(\mathbf{X}_j \mathbf{H}_i\right) + \tau_{j\notin v}\right) \tag{24}$$

Also, the constraint Eq.(12a) can be written as follows:

$$\gamma_j \geq Tr\left(\mathbf{X}_j\right) \tag{25}$$

By changing the variable $\phi_{ij}^2 = \varepsilon_{ij}$, the constraint $(10a)$ will be non-convex versus the variables $\left(\phi_{ij}, \tau_i\right)$ as it is not a perspective of function $\log\left(1 + x\right)$ anymore. In addition, any optimization problem that includes a $\log$ function, will turn the problem into a not disciplined convex problem and cannot be efficiently solved using modern semi-definite programming (SDP) solvers, such as SeDuMi [56]. To overcome this problem, new solutions called sequential quadratic (SQ) and conic quadratic representation (CQR) methods are proposed that will be described in subsections C and D.

*C. Sequential Quadratic (S.Q)*

An auxiliary $\theta_i$ variable is defined to convert the constraint $a)$ of Eq.(10) to the two following inequalities:

$$a_1)\ \theta_i \leq \frac{|g_i|^2}{\sigma_{UE}^2}\sum_{j=1, j\notin v}^{J}\phi_{ij}^2 \qquad i, j \in \mathbf{\Psi} \tag{26}$$

$$a_2)\ C_i - \tau_{j\in v}\log_2\left(1 + \frac{\theta_i}{\tau_{j\in v}}\right) \le 0 \quad i \in \mathbf{\Psi} \tag{27}$$

The relation $a_1)$ is not convex and should be using the difference between the convex functions method and linearization of the second part by the first-order approximation. As mentioned in the previous sections, replacing the linear approximation around the initial point, in the second part of Eq.(26):

$$\hat{a}_1)\ \theta_i - \frac{|g_i|^2}{\sigma_{UE}^2}\left(\sum_{j=1,j\notin v}^J \hat{\phi}_{ij}^2 + 2\left(\phi_{ij} - \hat{\phi}_{ij}\right)\sum_{j=1,j\notin v}^J \hat{\phi}_{ij}\right) \le 0 \tag{28}$$

Also, the constraint $a_2)$ is convex; however, it is not disciplined due to the logarithm function. One approach for turning it into a disciplined form is to find an upper bound approximation by quadratic form and apply the inner approximation. The following theorem gives an iterative approach similar to inner approximation which converges to the local optimum for a smooth optimization problem.

**Theorem**: the function $f_3 : D \to \mathbb{R},\ \forall x, \hat{x} \in D$ , is convex if a second derivative exists at each point in domain $D$ and $\nabla^2 f_3(\hat{x}) \ge 0$, hence, the second-order approximation is [57]:

$$f_3(x) = f_3(\hat{x}) + \nabla f_3(\hat{x})(x - \hat{x})^T + (x - \hat{x})\nabla^2 f_3(\hat{x})(x - \hat{x})^T \tag{29}$$

According to the above relation, the matrix $\mathbf{H_s}$ (called an upper bound Hessian matrix) must satisfy the following relation:

$$\nabla^2 f_3(\hat{x}) \preceq \mathbf{H_s} \tag{30}$$

If the above relation is established, Eq.(29) can be converted as follows:

$$f_3(x) \le f_3(\hat{x}) + \nabla f_3(\hat{x})(x - \hat{x})^T + (x - \hat{x})\mathbf{H_s}(x - \hat{x})^T \tag{31}$$

where the function $f_3$ is defined as the left-hand side of the constraint $a_2)$ .the value of $\nabla^2 f_3(\hat{x})$ can be obtained as follows:

$$\nabla^2 f_3(\theta_i, \tau_{j\in v}) = \begin{bmatrix} \frac{\tau_{j\in v}}{(\tau_{j\in v}+\theta_i)^2} & -\frac{\theta_i}{(\tau_{j\in v}+\theta_i)^2} \\ -\frac{\theta_i}{(\tau_{j\in v}+\theta_i)^2} & \frac{\theta_i^2}{\tau_{j\in v}(\tau_{j\in v}+\theta_i)^2} \end{bmatrix} \tag{32}$$

Matrix $\nabla^2 f_3(\theta_i, \tau_{j\in v})$ for $\tau_{j\in v}, \theta_i \ge 0$ does not have an upper bound. Therefore, we consider the below feasible set to bound it ($\beta$ is a fixed number):

$$D_i = \left\{(\theta_i, \tau_{j\in v})|\ \theta_i \ge 0, 0 \le \frac{\hat{\tau}_{j\in v}}{\beta} \le \tau_{j\in v} \le \infty\right\} \tag{33}$$

This new domain, which is an implicit constraint, is added to the constraints of the main problem. Now to estimate an upper bound of Eq.(32), the following matrix is replaced instead of it (see the proof of this, in the appendix):

$$\nabla^2 f_3\left(\theta_i, \tau_{j\in v}\right) \leq \begin{bmatrix} \frac{9\beta}{8\hat{\tau}_{j\in v}} & -\frac{\beta}{8\hat{\tau}_{j\in v}} \\ -\frac{\beta}{8\hat{\tau}_{j\in v}} & \frac{9\beta}{8\hat{\tau}_{j\in v}} \end{bmatrix} \leq \mathbf{H_s} \tag{34}$$

Also, the gradient of Eq.(27) is as follows:

$$\nabla f_3\left(\theta_i, \tau_{j\in v}\right) = \left[ -\frac{\tau_{j\in v}}{\tau_{j\in v}+\theta_i}, -\log\left(1+\frac{\theta_i}{\tau_{j\in v}}\right) + \frac{\theta_i}{\tau_{j\in v}+\theta_i} \right] \tag{35}$$

Therefore, according to Eqs.(29),(34) and (35), the $a_2$) constraint is converted to:

$$\hat{a}_2) \, C_i - \hat{\tau}_{j\in v}\log_2\left(1+\frac{\hat{\theta}_i}{\hat{\tau}_{j\in v}}\right) + \nabla f_3\left(\hat{\theta}_i, \hat{\tau}_{j\in v}\right)\left[\theta_i - \hat{\theta}_i, \tau_{j\in v} - \hat{\tau}_{j\in v}\right]^T$$
$$+ \left[\theta_i - \hat{\theta}_i, \tau_{j\in v} - \hat{\tau}_{j\in v}\right]\mathbf{H_s}\left[\theta_i - \hat{\theta}_i, \tau_{j\in v} - \hat{\tau}_{j\in v}\right]^T \leq 0 \tag{36}$$

Finally, according to Eqs.(10), (12), (13), (14), (17), (21), (24), (25), (28), (33) and (36), the final convex optimization for the SQ approach is obtained as follows:

$$\min_{\substack{\tau_j, \mathbf{X}_j, \gamma_j \\ \phi_{ij}, \theta_i}} \mathrm{E_T} = \sum_{j=1}^{J} \begin{pmatrix} \frac{1}{4}\left(\tau_j + \gamma_j\right)^2 - \frac{1}{4}\left(\hat{\tau}_j - \hat{\gamma}_j\right)^2 - \frac{1}{2}\left(\hat{\tau}_j - \hat{\gamma}_j\right)\left(\left(\tau_j - \gamma_j\right) - \left(\hat{\tau}_j - \hat{\gamma}_j\right)\right) + \\ \ell\left(Tr\left(\mathbf{X}_j\right) - \mathbf{v}_{\max}^H\left(\hat{\mathbf{X}}_j\right)\mathbf{X}_j\mathbf{v}_{\max}\left(\hat{\mathbf{X}}_j\right)\right) \end{pmatrix}$$
$$\text{s.t.} \quad (10b), (10c), (17b), (24), (25), (28), (33), (36) \tag{37}$$

Now this problem is discipline and convex. So, the optimal value of variables and objective function for the SQ approach is obtained by the algorithm 1.

*D. Conic Quadratic Representation (CQR)*

An auxiliary variable $z_i$ is introduced to convert the constraint $a)$ to the two following inequalities:

$$a_1)z_i \geq \frac{C_i}{\tau_{j\in v}} \quad , i \in \mathbf{\Psi} \tag{38}$$

$$a_2)\log_2\left(1 + \frac{|g_i|^2}{\tau_{j\in v}\sigma_{UE}^2}\sum_{j=1, j\notin v}^{J}\phi_{ij}^2\right) \geq z_i, i \in \mathbf{\Psi} \tag{39}$$

To use the above constraints in the main optimization problem, first, we need to ensure that these equations are convex and disciplined. Therefore, some changes should be applied to them (consider $\tau_j, z_i \geq 0, i \in \mathbf{\Psi}$):

$$z_i \geq \frac{C_i}{\tau_{j\in v}} \rightarrow \left(z_i + \tau_{j\in v}\right)^2 \geq 4C_i + \left(z_i - \tau_{j\in v}\right)^2 \tag{40}$$

---

**Algorithm 1** Sequential Quadratic (S.Q)

---

1- Initialize $\hat{\mathbf{X}}_j, \hat{\phi}_{ij}, \hat{\tau}_j, \hat{\gamma}_j, \hat{\theta}_i, \beta, a$ in the feasible set

2- Choose $\varepsilon \geq 0, \eta \geq 0$

3- **While** $counter < counter_{\max}$

4-  Solve (37) to obtain the solution variables $\mathbf{X}_j, \phi_{ij}, \tau_j, \gamma_j, \theta_i$

5-  **IF** $\left\{ \left\| \mathbf{X}_j - \hat{\mathbf{X}}_j \right\|, \left\| \phi_{ij} - \hat{\phi}_{ij} \right\|, \left\| \tau_j - \hat{\tau}_j \right\|, \left\| \gamma_j - \hat{\gamma}_j \right\|, \left\| \theta_i - \hat{\theta}_i \right\| \right\} > \varepsilon$

6-    $\mathbf{X}_j \to \hat{\mathbf{X}}_j, \phi_{ij} \to \hat{\phi}_{ij}, \tau_j \to \hat{\tau}, \gamma_j \to \hat{\gamma}_j, \theta_i \to \hat{\theta}_i$

7-    Go to step 3

8-  **Else**

9-    Check the the Rank one constraint Eq.(18) to be satisfied by $\frac{\text{Tr}(\mathbf{X}_j) - \lambda_{\max}(\mathbf{X}_j)}{\text{Tr}(\mathbf{X}_j)} \leq \varepsilon$

10-   $counter \to counter + 1$

11-   **IF** the constraint is not satisfied in Step 9

12-    then set $\alpha\ell \to \ell$ and go to Step 3

13-   **Else**

14-    $(\mathbf{X}_{opt}, \phi_{opt}, \tau_{opt}, \gamma_{opt}, \theta_{opt}) = (\mathbf{X}_j, \phi_{ij}, \tau_j, \gamma_j, \theta_i)$

15-   **End IF**

16-  **End IF**

17- **End While**

---

Since $z_i, \tau_i \geq 0$ , the above CQR relation can be written as follows:

$$(z_i + \tau_{j \in v}) \geq \left\| \left[ 2\sqrt{C_i}, (z_i - \tau_{j \in v}) \right] \right\|_2 \tag{41}$$

To simplify the inequality Eq.(39), the new auxiliary variable $\Xi_i$ , $i \in \mathbf{\Psi}$ is defined:

$$\Xi_i \leq \frac{|g_i|^2 \sum\limits_{j=1, j \notin v}^{J} \phi_{ij}^2}{\tau_{j \in v} \sigma_{UE}^2} \quad , \quad i \in \mathbf{\Psi} \tag{42}$$

Therefore

$$1 + \Xi_i \geq e^{z_i}, \ i \in \mathbf{\Psi} \tag{43}$$

The constraint of Eq.(43) is non-convex. In general, to solve the above relation, it is needed to approximate it with the following lemma.

**Lemma**: If a set of auxiliary variables $\zeta_{q,i}, q \in \{1, ..., M+4\}, i \in \boldsymbol{\Psi}$ satisfy the following inequalities, then we can use the CQR method to approximate the equivalent of the $1 + \Xi_i \geq e^{z_i}, \; i \in \boldsymbol{\Psi}$ with is the following linear and conic inequalities.

$$1 + \Xi_i \geq \zeta_{M+4,i}, \qquad\qquad i \in \boldsymbol{\Psi} \qquad (44a)$$

$$1 + \zeta_{1,i} \geq \left\| \left[ \begin{array}{cc} 1 - \zeta_{1,i} & 2 + 2^{1-M} z_i \end{array} \right] \right\|_2, \qquad i \in \boldsymbol{\Psi} \qquad (44b)$$

$$1 + \zeta_{2,i} \geq \left\| \left[ \begin{array}{cc} 1 - \zeta_{2,i} & 5/3 + 2^{-M} z_i \end{array} \right] \right\|_2, \qquad i \in \boldsymbol{\Psi} \qquad (44c)$$

$$1 + \zeta_{3,i} \geq \left\| \left[ \begin{array}{cc} 1 - \zeta_{3,i} & 2\zeta_{1,i} \end{array} \right] \right\|_2, \qquad i \in \boldsymbol{\Psi} \qquad (44d)$$

$$\zeta_{4,i} \geq \zeta_{2,i} + \zeta_{3,i}/24 + 19/72, \qquad\qquad i \in \boldsymbol{\Psi} \qquad (44e)$$

$$1 + \zeta_{q,i} \geq \left\| \left[ \begin{array}{cc} 1 - \zeta_{q,i} & 2\zeta_{q-1,i} \end{array} \right] \right\|_2, \qquad q \in \{5, ..., M+4\}, i \in \boldsymbol{\Psi} \qquad (44f)$$

The accuracy of the approximation increases with $M$, where the suitable value of $M$ is determined in such a way that the problem reaches convergence and has the least complexity at that point. Therefore, $M$ is called the approximation coefficient.

**Proof**: See [6], [58]

To establish a relation between the variables $\phi_{ij}^2$ and $\Xi_i$ the linear approximation for the right-hand side of Eq.(42) should be written similar to previous sections. By placing it in Eq.(42), the new constraint is obtained as follows and should be added to other constraints of the main problem (Eq.(12)):

$$\Xi_i - \frac{|g_i|^2}{\sigma_{UE}^2} \left( \frac{\sum_{j=1,j\notin v}^{J} \hat{\phi}_{ij}^2}{\hat{\tau}_{j\in v}} + \frac{2\phi_{ij} - \hat{\phi}_{ij} \sum_{j=1,j\notin v}^{J} \phi_{ij}}{\hat{\tau}_{j\in v}} - \frac{\tau_{j\in v} - \hat{\tau}_{j\in v} \sum_{j=1,j\notin v}^{J} \phi_{ij}^2}{\hat{\tau}_{j\in v}^2 \sigma_{UE}^2} \right) \leq 0 \qquad (45)$$

Finally, according to Eqs, (10), (12), (13), (14), (17), (21), (24), (25), (41), (44) and (45), the final convex optimization for the CQR approach is obtained as follows:

$$\min_{\substack{\tau_j, \mathbf{X}_j, \gamma_j, z, i \\ \Xi_i, \phi_{ij}, \zeta_{q,i}}} \mathrm{E_T} = \sum_{j=1}^{J} \left( \begin{array}{l} \frac{1}{4}(\tau_j + \gamma_j)^2 - \frac{1}{4}(\hat{\tau}_j - \hat{\gamma}_j)^2 - \frac{1}{2}(\hat{\tau}_j - \hat{\gamma}_j)((\tau_j - \gamma_j) - (\hat{\tau}_j - \hat{\gamma}_j)) + \\ \ell\left(Tr(\mathbf{X}_j) - \mathbf{v}_{\max}^H(\hat{\mathbf{X}}_j) \mathbf{X}_j \mathbf{v}_{\max}(\hat{\mathbf{X}}_j)\right) \end{array} \right)$$

$$\text{s.t.} \quad (10b), (10c), (17b), (24), (25), (41), (44), (45)$$

$$(46)$$

Now this problem is discipline and convex. So, the optimal value of variables and objective function for the CQR approach is obtained by the algorithm 2.

The advantage of the CQR method is to obtain the optimal solution by increasing the value of the coefficient of approximation (M). At the end of this calculation and after obtaining $\mathbf{X}_j$, the variable $\mathbf{x}_j$ is obtained according to Equation $\mathbf{X}_j = \mathbf{x}_j \mathbf{x}_j^H$.

---

**Algorithm 2** Conic Quadratic Representation (CQR)

---

1- Initialize $\hat{\mathbf{X}}_j, \hat{\phi}_{ij}, \hat{\tau}_j, \hat{\gamma}_j, \alpha, M$ in the feasible set

2- Choose $\varepsilon \geq 0, \eta \geq 0$

3- **While** $counter < counter_{\max}$

4-   Solve (46) to obtain the solution variables $\mathbf{X}_j, \phi_{ij}, \tau_j, \gamma_j, \Xi_i, \xi_{M+4,i}, z_i$

5- **IF** $\left\{ \left\| \mathbf{X}_j - \hat{\mathbf{X}}_j \right\|, \left\| \phi_{ij} - \hat{\phi}_{ij} \right\|, \| \tau_j - \hat{\tau}_j \|, \| \gamma_j - \hat{\gamma}_j \| \right\} > \varepsilon$

6-     $\mathbf{X}_j \to \hat{\mathbf{X}}_j, \phi_{ij} \to \hat{\phi}_{ij}, \tau_j \to \hat{\tau}, \gamma_j \to \hat{\gamma}_j$

7-     Go to step 3

8- **Else**

9-     Check the the Rank one constraint Eq.(18) to be satisfied by $\frac{\text{Tr}(\mathbf{X}_j)\text{-}\lambda_{\max}(\mathbf{X}_j)}{\text{Tr}(\mathbf{X}_j)} \leq \varepsilon$

10-    $counter \to counter + 1$

11-    **IF** the constraint is not satisfied in Step 9

12-       then set $\alpha\ell \to \ell$ and go to Step 3

13-    **Else**

14-       $(\mathbf{X}_{opt}, \phi_{opt}, \tau_{opt}, \gamma_{opt}) = (\mathbf{X}_j, \phi_{ij}, \tau_j, \gamma_j)$

15-    **End IF**

16-  **End IF**

17- **End While**

---

## IV.  COMPLEXITY BOUND

In this section, the complexity bounds are calculated based on the interior-point method [59] for proposed optimization problems. Interior point methods were extended from linear optimization to semi-definite optimization and the polynomial complexity of the algorithm can be obtained theoretically [60]. In this method, the number of accuracy digits in an $\varepsilon$-solution is defined as $Digits(p, \varepsilon) \approx Ln\left(size\left(p\right)/\varepsilon\right)$ where $size(p)$ is the dimension of the total data of the problem $p$, and $p$ can be the CQR or S.Q problems.

After the calculations of the complexity, the size of the CQR problem is $6I^4 + (6N^4 + 9M + 80)I^3$ and its complexity is $\mathcal{O}\left[I^6\left(20I + 42N^4 + 50M\right) \times Ln\left(size\left(CQR\right)/\varepsilon\right)\right]$. In the S.Q problem, size and complexity is $6I^4 + (6N^4 + 32)I^3$ and $\mathcal{O}\left[(20I^7 + 42N^4I^6) \times Ln\left(size\left(S.Q\right)/\varepsilon\right)\right]$ respectively. It should be noted that since the computational load related to the complexity of these methods is very high, only the approximate final values are considered in the above

relations. To better understand the complexity of these methods, and since the relations may be complex to make sense, the corresponding figure is drawn in the simulation section by using the exact results of the calculations.

## V. COMPARISON AN EE OF SR SYSTEM WITH OTHER IOT PROTOCOLS

In a 6G and B5G networks, the operating frequency is very high and therefore the distance between cells is very short and the uncovered areas are numerous in the network. These challenges can be almost solved with the help of different scenarios such as relays, small cells, cell-free systems and intelligent reflect surface, but the cost of implementation of these structures is high. A more appropriate and newer solution is to use the SR system. The SR system is suitable for establishing communications between IoT users and cellular networks. In case there are many Iot users in the network, only the use of structures similar to the SR system can provide the desired QoS in the future networks. Because, as mentioned in the previous sections, the SR system has many advantages such as no need for infrastructure, increased spectral efficiency, and increased EE, which was examined in this article, the third case.

The SBDs in the SR system can be used in two cases; The first is the case, where the SBDs themselves have information to send, similar to the environmental sensors used in the network, which is discussed in this paper; Second, the SBDs themselves do not have information and just like a relay network transmits the information of a sender to intended destinations.

If the data interference in receivers can be ignored, the two above proposed cases of SR can be implemented with some other IoT protocols; such as cooperative relay and sensor networks which using the batteries (e.g., LoRa, ZigBee, ...), or sensors with wirelessly energy harvesting in the wireless powered communication networks (WPCN). These systems, in addition to using active energy consuming components such as ADC, processor, power amplifier, etc., require a complex electrical and communication infrastructure to send their information. On the other hand, in the SR system, SBDs use a particular structure [27] with the EC being close to zero, and also the transceiver antenna being passive. SBDs also pick up this limited energy from the ambient signals. In this section, we intend to compare the EC in a cell with a large number of sensors that can be implemented with different systems such as SR, LpWan, and ZigBee, regardless of the EC of the active base station cells.The values related to the EC of each system are given in Table I, where the EC related to the infrastructure of each system is ignored. Also, the corresponding diagram is drawn in the simulation section.

TABLE I:

Energy Consumption of SR and IoT protocols for one IoT device and in one transmission slot.

| IoT protocols | Energy Consumption | Reference |
|:---:|:---:|:---:|
| SigFox | $\sim 0.2J$ | [2], [61]–[64] |
| LoRa | $\sim 0.04J$ | |
| NB-IoT | $\sim 0.062J$ | |
| ZigBee | $\sim 1.4J$ | [2], [65] |
| SR | $\sim 0.015J$ | This Paper |

## VI. SIMULATION RESULTS

According to the system model, SBDs, which can be IoT devices, are randomly distributed in the network and almost near the SUE. Each IoT device can harvest energy and send its information to the intended SUE, as shown in Fig.1. We consider the sum of all time slots in each transition period frame by BSs is $T = 10$ and $\eta = 0.8$ and also $\sigma_i^2 = \sigma_{UE}^2$ was considered. All simulation results were obtained by averaging over 200 randomly generated channels on downlink harvest energy and uplink information transmission in SBDs. Also, ten different initialization points in the convex feasible set were considered to ensure the stability of the problems.

### A. Comparison of Proposed Methods

In this paper, two mathematical methods were used to solve the optimization problem called CQR and S.Q. In the CQR method, the first step is to obtain the appropriate approximation coefficient; therefore, the diagram of the minimum energy transfer (consumption) by BSs versus SBDs throughput requirement in Fig.3 is plotted by assuming approximation coefficients as $M = 1, 2, ..., 6$ in the CQR method. In Fig.3, as expected, with increasing the minimum data transmission rate in SBDs, the total EC in the network transferred by the BSs is also increased. As mentioned, the best approximation coefficient must be found for this problem, where the shapes converge to each other. Based on Fig.3, for $M \geq 4$ this event occurs and so the appropriate values are obtained. The optimal value will be obtained by considering the computational complexity according to Fig. 6, and this value is equal to $M = 4$.
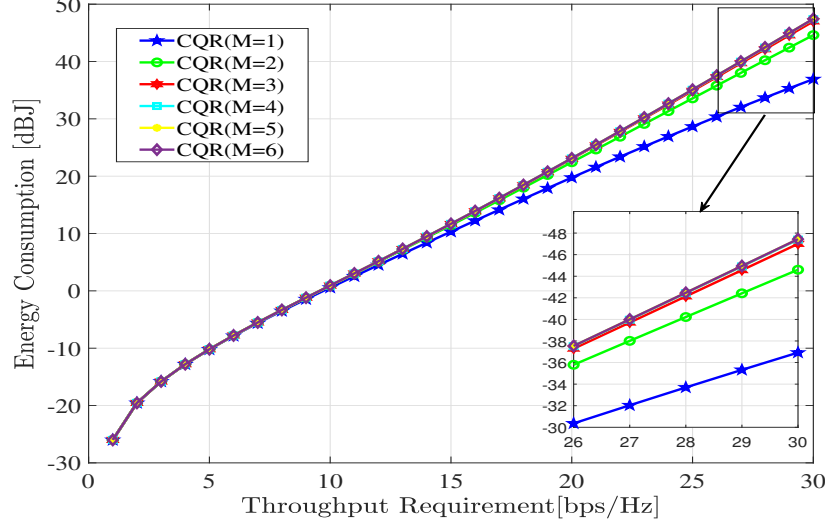
Fig. 3: EC versus SBDs throughput requirement in CQR method for $M = 1, 2, ..., 6$, $I = 6$

Now, two methods that are CQR with $M = 4$ and SQ are compared with each other to see which of these mathematical solutions is more accurate in finding the optimal points. For this case, we change the basic parameters of the network design. One of the important basic parameters is the number of IoT devices in the network; hence, the minimum energy transfer versus SBDs throughput requirement for these two methods is depicted in Fig.4 where the number of SBDs varies from 2 to 4 ($I \in \{2, 3, 4\}$).

In the special case (for example, in $I = 3$), we see that the CQR is the better method to find optimization variables to minimize the total amount of EC in the network by taking into account the fulfillment of the SBDs throughput requirements.

Fig. 5 shows the effect of increasing the number of SBDs in each cell, on the amount of EC in the network, which grows dramatically with the increasing number of SBDs. The EC in two cases of 2 SBDs and 4 SBDs in the SQ method at rate 9 bps/Hz, differs 29dB and in the CQR method this difference equals to 7dB. Therefore, stability and EC in the CQR method are much better than in the SQ method with increasing the number of SBDs.

Another important parameter is the change in the number of energy output antennas on BSs. So, Fig.5 shows this for several antennas in each BS which is a single antenna, $2 \times 2$ and $3 \times 3$ antennas. It is observed that, with increasing the number of antennas in each BS, the amount of energy consumed in the network is decreased. This is because that, the energy is sent to users with narrower beams with a higher power level and hence, the energy losses will reduce and
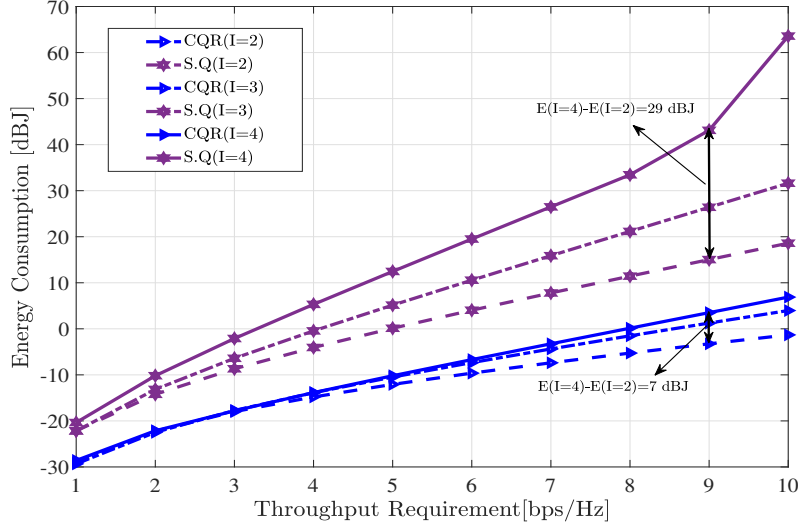
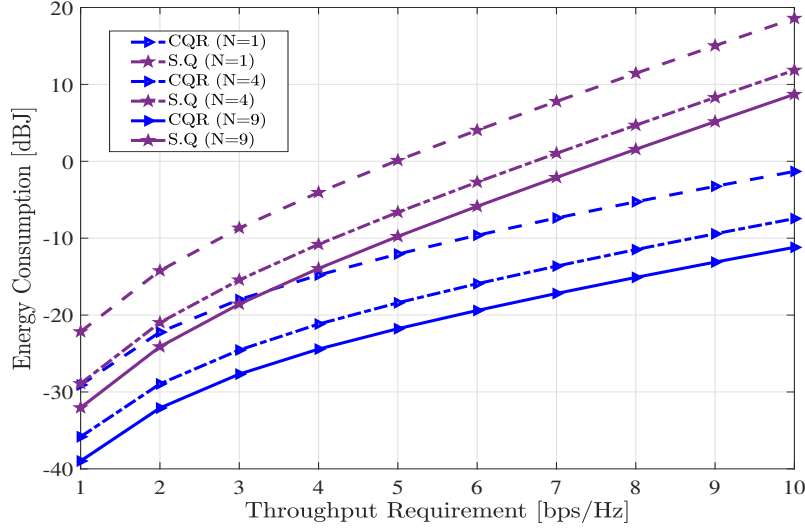Fig. 4: EC versus SBDs throughput requirement where the number of SBDs is $I = 2, 3, 4$



Fig. 5: EC versus SBDs throughput requirement where the number of BSs antennas is $N_s = 1, 4, 9$

the SBD batteries charge quickly; therefore, energy waste is significantly reduced.

### B. Computational Complexity

The simulation of the computational complexity of the SQ and CQR methods, which is presented in Section IV, is shown in Fig. 6. In this figure, the number of IoT devices (SBDs) is considered a variable. According to Fig.6, the computational complexity of the CQR method is greater than the S.Q method. Also, in the CQR, with increasing the value of $M$, the algorithm's complexity grows.
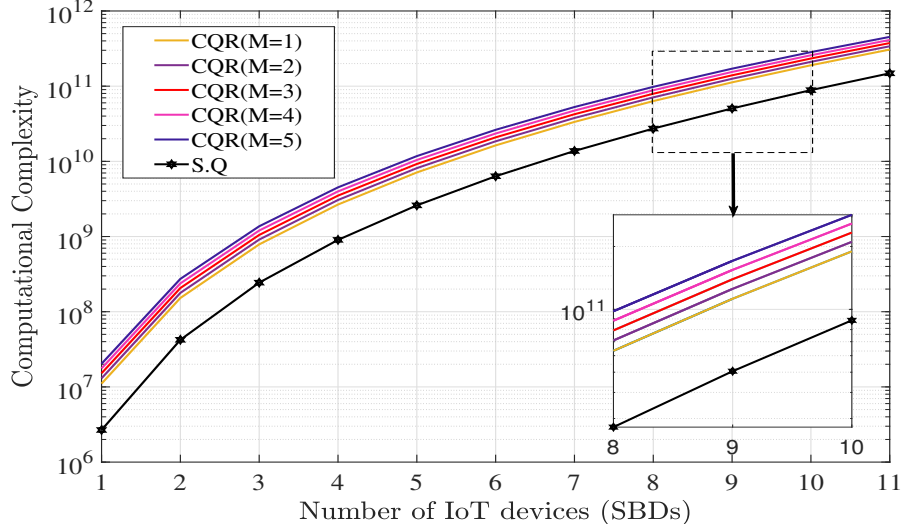
Fig. 6: The computational complexity of investigated methods where the number of SBDs changes from 1 to 11, $N = 4$ and $\varepsilon = 10^{-6}$

According to Fig.6 and descriptions of the previous sections, in the CQR method, the appropriate approximation coefficient where there is the least complexity and the best convergence in the function is $M = 4$.

## C. Comparison of T-SR and TDMA Modes

After proposing and simulating the SR system to decrease EC in B5G and 6G networks, we intend to compare the scheduling of this system, which was introduced as T-SR with the TDMA scheduling system.

Same as the T-SR mode which was shown in Fig.2, we draw the TDMA mode in Fig.7.

In the TDMA mode, SBDs take turns in transmitting their information in equal time slots in time frames [39]. If the amount of information sent in an SBD is large, it is necessary to allocate more slots to those SBDs.

Hereupon, in TDMA mode SBDs may transmit their data discontinuously in more than one-time frame, while in the T-SR mode the transmission data can be completed in one frame and with sequential time slots. The reason is, in TDMA, SBDs only have to send their data in the time slot allocated in that frame.

The T-SR mode is formulated as an SR system, which is the proposed system in this paper. According to the definitions, the TDMA scheme can be considered as a simplified case of T-SR and can be modeled by applying some simplifications to the T-SR model.

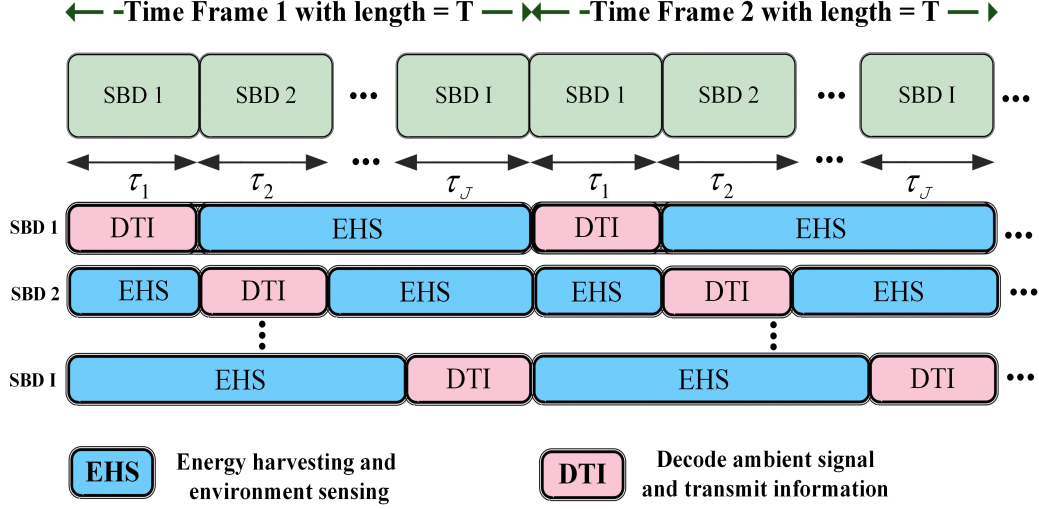← -Time Frame 1 with length = T — ←─ -Time Frame 2 with length = T — ▶



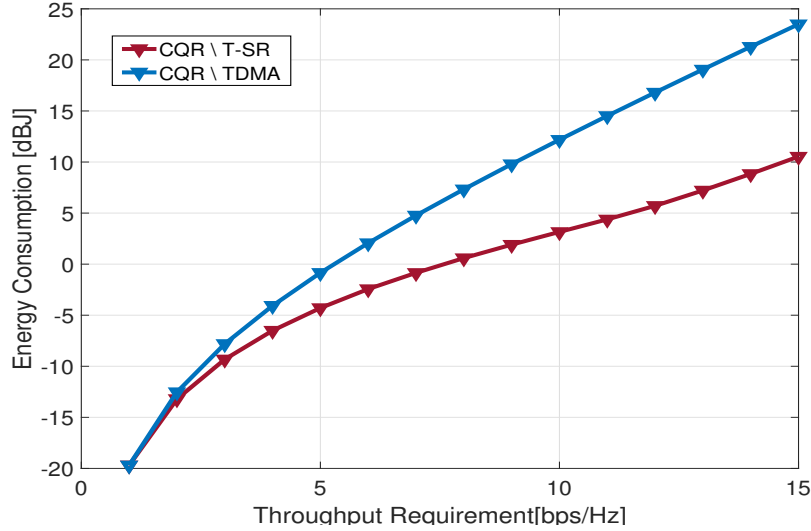Fig. 7: The TDD transmission frame for EHS and DTI modes in TDMA transmission information mode



Fig. 8: Comparison of the EC versus SBDs throughput requirement for the T-SR and TDMA scenarios, $I = 8, N = 9$

In this paper, the TDMA mode is simulated by assuming that it is well implemented in the network and in the receivers no interference occurs. Fig.8 compares the EC of the T-SR mode in the SR network and TDMA mode in typical networks which is presented in Fig.2 and Fig.7, respectively.

It is noted that the main purpose of this study is to minimize the amount of energy consumed in the network. According to Fig.8, the EC in the T-SR consumes much less energy than in the TDMA mode (about 8 dB). This is due to the optimal allocation of time slots according to the
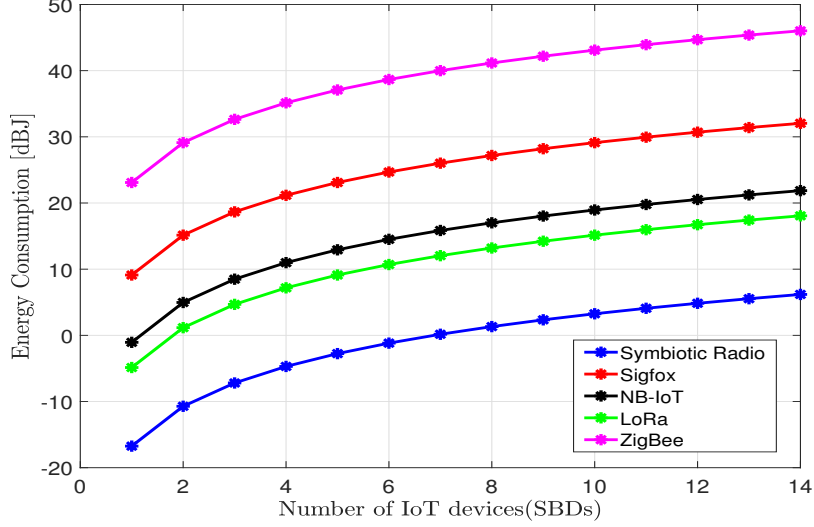
Fig. 9: EC comparison between IoT protocols and SR system against the number of IoT devices in each cell

needs of each SBDs as well as the ability to send information and harvest energy at any time. The difference between the EC of these two systems will increase if the volume of information sent is large and more time slots are needed to send it.

In section V and based on the table I, we compare the EC of the proposed method in this paper with other IoT communication protocols drawn in Fig.9. According to Fig.9, the power consumption of the SR system is lower than other IoT protocols. This comparison is performed in a situation where two SR features are ignored. The first, is the devices are using the passive components in the SR and the second is that there is no need to network infrastructure for the SR system. In the real world, both should be considered, which means the power consumption for the SR is much lower than that shown in the Fig.9.

## VII. CONCLUSION AND FUTURE WORK

This paper investigated the optimal time and power allocation with novel techniques in the symbiotic radio system for minimizing the EC in a network while satisfying the SBDs throughput requirement. Multiple SBDs harvest energy from ambient signals radiated from BSs and if they have information to send, after decoding the signal received from BS, they put the information on the carrier of that signal and send it to the intended SUE. To achieve the goal of the article, which is to minimize EC in high-density user networks such as B5G and 6G networks, a new technology without infrastructure and passive called SR has been used. In the SR system, TDMA

and timing in SR methods are introduced for scheduling data transmission between SBDs. We formulated the SR system that was a non-convex optimization problem and managed to solve it. The problem becomes a convex and disciplined problem using novel mathematical methods called CQR and S.Q. By comparing these two methods, we observed that the CQR method has better EE. Moreover, by changing the basic parameters of the network such as the number of IoT devices and the number of active massive MIMO antenna in BSs, CQR was stable and could further reduce EC in the network. In Fig. 8, we also compared the timing of this proposed system with the TDMA mode (in the SR system), which has a better EE for the reasons explained in the simulation section. Fig.9, presented the power consumption of a network with a large number of IoT users. When they use SR communications, the power consumption of the network is much lower than other current IoT communication protocols. This will have a huge impact to reduse the EC in the future generation networks on a global scale.

There are many ideas for future work, including investigating the spectral efficiency of the proposed system model in this paper, using the intelligence reflect surface (IRS), which is passive structure and will have a great impact on reducing the amount of EC and enhancing spectral and energy efficiency in the network and using the reinforced learning to reduce the EC in the dense IoT networks.

## APPENDIX

**Lemma**: The inequality $g\left(\theta_i, \tau_i\right) \leq g\left(\left(\theta_i, \tau_i\right), \left(\hat{\theta}_i, \hat{\tau}_i\right)\right)$ holds for $(\theta_i, \tau_i) \in \left\{(\theta_i, \tau_i) | \theta_i \geq 0, 0 \leq \frac{\hat{\tau}_i}{\beta} \leq \tau_i \leq \infty\right\}$, where $g\left(\theta_i, \tau_i\right) = \tau_i \log\left(1 + \frac{\theta_i}{\tau_i}\right)$ and $g\left(\left(\theta_i, \tau_i\right), \left(\hat{\theta}_i, \hat{\tau}_i\right)\right)$ is equal to: $\hat{\tau}_i \log\left(1 + \frac{\hat{\theta}_i}{\hat{\tau}_i}\right) + \nabla f\left(\hat{\theta}_i, \hat{\tau}_i\right)\left[\theta_i - \hat{\theta}_i, \tau_i - \hat{\tau}_i\right]^T + \left[\theta_i - \hat{\theta}_i, \tau_i - \hat{\tau}_i\right] \mathbf{H_s}\left[\theta_i - \hat{\theta}_i, \tau_i - \hat{\tau}_i\right]^T$

**Proof**: We first obtain the minimal matrix $\mathbf{A}$ which satisfies the following relation for $(\theta_i, \tau_i)$:

$$\mathbf{H_s} = \begin{bmatrix} \frac{\tau_i}{(\tau_i + \theta_i)^2} & -\frac{\theta_i}{(\tau_i + \theta_i)^2} \\ -\frac{\theta_i}{(\tau_i + \theta_i)^2} & \frac{\theta_i^2}{\tau_i(\tau_i + \theta_i)^2} \end{bmatrix} \leq \mathbf{A} = \begin{bmatrix} a_{11} & a_{12} \\ a_{21} & a_{22} \end{bmatrix} \tag{47}$$

According to Eq.(33) the largest value of $a_{11}$ is obtained when $\theta_i$ and $\tau_i$ have their lowest values

$$a_{11} = \arg\max_{\theta_i, \tau_i}\left\{\tau_i / (\tau_i + \theta_i)^2\right\} \Bigg|_{\substack{\theta_i = 0 \\ \tau_i = \hat{\tau}_i/\beta}} = \beta/\hat{\tau}_i \tag{48}$$

To obtain the maximum value of $a_{22}$ based on the function $\frac{\theta_i^2}{\tau_i(\tau_i + \theta_i)^2}$ is monotonically increasing with respect to $\theta_i$ and monotonically decreasing with respect to $\tau_i$:

$$a_{22} = \arg\max_{\theta_i, \tau_i}\left\{\frac{\theta_i^2}{\tau_i(\tau_i + \theta_i)^2}\right\} \Bigg|_{\substack{\text{Lim}\,\theta_i \to \infty \\ \tau_i = \hat{\tau}_i/\beta}} = \beta/\hat{\tau}_i \tag{49}$$

To obtain $a_{21} = a_{12}$, the derivative of the function $\frac{\theta_i}{(\tau_i+\theta_i)^2}$ is calculated and it is observed that the maximum value of this function is obtained for $\tau_i = \theta_i$ and also $\tau_i$ has it's lowest value, so:

$$a_{12} = a_{21} \leq \underset{\theta_i,\tau_i}{\arg\max} \left\{ \frac{\theta_i}{(\tau_i + \theta_i)^2} \right\} \Bigg|_{\substack{\theta_i = \hat{\tau}_i/\beta \\ \tau_i = \hat{\tau}_i/\beta}} = \beta/4\hat{\tau}_i \tag{50}$$

In addition, to satisfy the above relations, the determinant of the matrix (47) is also greater than zero. By defining an auxiliary variable $\Re$ , this inequality will be simplified as follows:

$$\underbrace{\left(a_{11} - \frac{\tau_i}{(\tau_i + \theta_i)^2}\right)}_{\Re_1} \underbrace{\left(a_{22} - \frac{\theta_i^2}{\tau_i(\tau_i + \theta_i)^2}\right)}_{\Re_2} - \underbrace{\left(a_{12} + \frac{\theta_i}{(\tau_i + \theta_i)^2}\right)^2}_{\Re} \geq 0 \tag{51}$$

Consequently, based on Eq.(51) we can calculate the $a_{21} = a_{12}$:

$$a_{12} = a_{21} = -\frac{1}{2}\left(\max\left(\frac{\theta_i}{(\tau_i+\theta_i)^2}\right) - \min\left(\frac{\theta_i}{(\tau_i+\theta_i)^2}\right)\right) = -\frac{1}{2}\left(\frac{\beta}{4\hat{\tau}_i} - 0\right) = -\frac{\beta}{8\hat{\tau}_i} \tag{52}$$

The following inequality is established for $\Re$ :

$$\Re \geq \left(-\frac{\beta}{8\hat{\tau}_i} + \frac{\beta}{4\hat{\tau}_i}\right) = \frac{\beta}{8\hat{\tau}_i} \tag{53}$$

and also, we have the following relationships:

$$a_{11} \leq \Re_1 + \frac{\beta}{\hat{\tau}_i} = \frac{9\beta}{8\hat{\tau}_i} \;, a_{22} \leq \Re_2 + \frac{\beta}{\hat{\tau}_i} = \frac{9\beta}{8\hat{\tau}_i} \tag{54}$$

Finally, after these calculations, an upper bound of matrix (32) is shown by Eq.(34).

## REFERENCES

[1] Q. Wu, X. Zhou, W. Chen, J. Li, and X. Zhang, "Irs-aided wpcns: A new optimization framework for dynamic irs beamforming," *IEEE Transactions on Wireless Communications*, 2021.

[2] R. K. Singh, P. P. Puluckul, R. Berkvens, and M. Weyn, "Energy consumption analysis of lpwan technologies and lifetime estimation for iot application," *Sensors*, vol. 20, no. 17, p. 4794, 2020.

[3] K. Lee and J. Ko, "Wireless information and power transfer: Probability-based power allocation and splitting with low complexity," *IEEE Systems Journal*, vol. 12, no. 1, pp. 1060–1064, 2016.

[4] Z. Ding, Y. Liu, J. Choi, Q. Sun, M. Elkashlan, I. Chih-Lin, and H. V. Poor, "Application of non-orthogonal multiple access in lte and 5g networks," *IEEE Communications Magazine*, vol. 55, no. 2, pp. 185–191, 2017.

[5] R. Oltman, "5g is coming: How t&m manufacturers can prepare for and benefit from 5g," *5G Semiconductor Solutions-Infrastructure and Fixed Wireless Access*, p. 19, 2018.

[6] T. P. Do and Y. H. Kim, "Resource allocation for a full-duplex wireless-powered communication network with imperfect self-interference cancelation," *IEEE Communications Letters*, vol. 20, no. 12, pp. 2482–2485, 2016.

[7] J. Cao, Z. Bu, Y. Wang, H. Yang, J. Jiang, and H.-J. Li, "Detecting prosumer-community groups in smart grids from the multiagent perspective," *IEEE Transactions on Systems, Man, and Cybernetics: Systems*, vol. 49, no. 8, pp. 1652–1664, 2019.

[8] Y. Luo, L. Pu, G. Wang, and Y. Zhao, "Rf energy harvesting wireless communications: Rf environment, device hardware and practical issues," *Sensors*, vol. 19, no. 13, p. 3010, 2019.

[9] X. Deng, Z. Tang, L. Yi, and L. T. Yang, "Healing multimodal confident information coverage holes in nb-iot-enabled networks," *IEEE Internet of Things Journal*, vol. 5, no. 3, pp. 1463–1473, 2017.

[10] S. S. Adhatarao, M. Arumaithurai, D. Kutscher, and X. Fu, "Isi: Integrate sensor networks to internet with icn," *IEEE Internet of Things Journal*, vol. 5, no. 2, pp. 491–499, 2017.

[11] P. Zhang, X. Kang, D. Wu, and R. Wang, "High-accuracy entity state prediction method based on deep belief network toward iot search," *IEEE Wireless Communications Letters*, vol. 8, no. 2, pp. 492–495, 2018.

[12] J. Hu, Q. Wang, and K. Yang, "Energy self-sustainability in full-spectrum 6g," *IEEE Wireless Communications*, vol. 28, no. 1, pp. 104–111, 2020.

[13] D. Niyato, D. I. Kim, M. Maso, and Z. Han, "Wireless powered communication networks: Research directions and technological approaches," *IEEE Wireless Communications*, vol. 24, no. 6, pp. 88–97, 2017.

[14] A. J. Williams, M. F. Torquato, I. M. Cameron, A. A. Fahmy, and J. Sienz, "Survey of energy harvesting technologies for wireless sensor networks," *IEEE Access*, vol. 9, pp. 77 493–77 510, 2021.

[15] T. Sanislav, S. Zeadally, G. D. Mois, and S. C. Folea, "Wireless energy harvesting: Empirical results and practical considerations for internet of things," *Journal of Network and Computer Applications*, vol. 121, pp. 149–158, 2018.

[16] T. Sanislav, G. D. Mois, S. Zeadally, and S. C. Folea, "Energy harvesting techniques for internet of things (iot)," *IEEE Access*, vol. 9, pp. 39 530–39 549, 2021.

[17] N. Su and Q. Zhu, "Power control and channel allocation algorithm for energy harvesting d2d communications," *Algorithms*, vol. 12, no. 5, p. 93, 2019.

[18] D. K. P. Asiedu, S. Mahama, S.-W. Jeon, and K.-J. Lee, "Optimal power splitting for simultaneous wireless information and power transfer in amplify-and-forward multiple-relay systems," *IEEE Access*, vol. 6, pp. 3459–3468, 2018.

[19] V. Liu, A. Parks, V. Talla, S. Gollakota, D. Wetherall, and J. R. Smith, "Ambient backscatter: Wireless communication out of thin air," *ACM SIGCOMM computer communication review*, vol. 43, no. 4, pp. 39–50, 2013.

[20] M. B. Janjua and H. Arslan, "Survey on symbiotic radio: A paradigm shift in spectrum sharing and coexistence," *arXiv preprint arXiv:2111.08948*, 2021.

[21] Z. Chen and B. Ji, "Resource allocation algorithm for iot communication based on ambient backscatter," in *2021 IEEE 93rd Vehicular Technology Conference (VTC2021-Spring)*. IEEE, 2021, pp. 1–5.

[22] L. Zhang, Y.-C. Liang, and M. Xiao, "Spectrum sharing for internet of things: A survey," *IEEE Wireless Communications*, vol. 26, no. 3, pp. 132–139, 2018.

[23] Z. Qin, X. Zhou, L. Zhang, Y. Gao, Y.-C. Liang, and G. Y. Li, "20 years of evolution from cognitive to intelligent communications," *IEEE transactions on cognitive communications and networking*, vol. 6, no. 1, pp. 6–20, 2019.

[24] Y.-C. Liang, K.-C. Chen, G. Y. Li, and P. Mahonen, "Cognitive radio networking and communications: An overview," *IEEE transactions on vehicular technology*, vol. 60, no. 7, pp. 3386–3407, 2011.

[25] Y.-C. Liang, Q. Zhang, E. G. Larsson, and G. Y. Li, "Symbiotic radio: Cognitive backscattering communications for future wireless networks," *IEEE Transactions on Cognitive Communications and Networking*, vol. 6, no. 4, pp. 1242–1255, 2020.

[26] G. Yang, Q. Zhang, and Y.-C. Liang, "Cooperative ambient backscatter communications for green internet-of-things," *IEEE Internet of Things Journal*, vol. 5, no. 2, pp. 1116–1130, 2018.

[27] N. Van Huynh, D. T. Hoang, X. Lu, D. Niyato, P. Wang, and D. I. Kim, "Ambient backscatter communications: A contemporary survey," *IEEE Communications surveys & tutorials*, vol. 20, no. 4, pp. 2889–2922, 2018.

[28] M. N. Mahdi, A. R. Ahmad, Q. S. Qassim, H. Natiq, M. A. Subhi, and M. Mahmoud, "From 5g to 6g technology: meets energy, internet-of-things and machine learning: a survey," *Applied Sciences*, vol. 11, no. 17, p. 8117, 2021.

[29] F. Qamar, M. U. A. Siddiqui, M. N. Hindia, R. Hassan, and Q. N. Nguyen, "Issues, challenges, and research trends in spectrum management: A comprehensive overview and new vision for designing 6g networks," *Electronics*, vol. 9, no. 9, p. 1416, 2020.

[30] C. Huang, S. Hu, G. C. Alexandropoulos, A. Zappone, C. Yuen, R. Zhang, M. Di Renzo, and M. Debbah, "Holographic mimo surfaces for 6g wireless networks: Opportunities, challenges, and trends," *IEEE Wireless Communications*, vol. 27, no. 5, pp. 118–125, 2020.

[31] S. Chen, Y.-C. Liang, S. Sun, S. Kang, W. Cheng, and M. Peng, "Vision, requirements, and technology trend of 6g: How to tackle the challenges of system coverage, capacity, user data-rate and movement speed," *IEEE Wireless Communications*, vol. 27, no. 2, pp. 218–228, 2020.

[32] S. J. Nawaz, S. K. Sharma, B. Mansoor, M. N. Patwary, and N. M. Khan, "Non-coherent and backscatter communications: Enabling ultra-massive connectivity in 6g wireless networks," *IEEE Access*, vol. 9, pp. 38 144–38 186, 2021.

[33] L. Bariah, L. Mohjazi, S. Muhaidat, P. C. Sofotasios, G. K. Kurt, H. Yanikomeroglu, and O. A. Dobre, "A prospective look: Key enabling technologies, applications and open research topics in 6g networks," *IEEE access*, vol. 8, pp. 174 792–174 820, 2020.

[34] A. Patil, S. Iyer, and R. J. Pandya, "A survey of machine learning algorithms for 6g wireless networks," *arXiv preprint arXiv:2203.08429*, 2022.

[35] Z. Dai, R. Li, J. Xu, Y. Zeng, and S. Jin, "Cell-free symbiotic radio: Channel estimation method and achievable rate analysis," in *2021 IEEE/CIC International Conference on Communications in China (ICCC Workshops)*. IEEE, 2021, pp. 25–30.

[36] R. Long, H. Guo, L. Zhang, and Y.-C. Liang, "Full-duplex backscatter communications in symbiotic radio systems," *IEEE Access*, vol. 7, pp. 21 597–21 608, 2019.

[37] R. Long, Y.-C. Liang, H. Guo, G. Yang, and R. Zhang, "Symbiotic radio: A new communication paradigm for passive internet of things," *IEEE Internet of Things Journal*, vol. 7, no. 2, pp. 1350–1363, 2019.

[38] Y. Xu, Z. Qin, G. Gui, H. Gacanin, H. Sari, and F. Adachi, "Energy efficiency maximization in noma enabled backscatter communications with qos guarantee," *IEEE Wireless Communications Letters*, vol. 10, no. 2, pp. 353–357, 2020.

[39] H. Yang, Y. Ye, K. Liang, and X. Chu, "Energy efficiency maximization for symbiotic radio networks with multiple backscatter devices," *IEEE Open Journal of the Communications Society*, vol. 2, pp. 1431–1444, 2021.

[40] Y. Liu, P. Ren, and Q. Du, "Symbiotic communication: Concurrent transmission for multi-users based on backscatter communication," in *2020 International Conference on Wireless Communications and Signal Processing (WCSP)*. IEEE, 2020, pp. 835–839.

[41] S. Han, Y.-C. Liang, and G. Sun, "The design and optimization of random code assisted multi-bd symbiotic radio system," *IEEE Transactions on Wireless Communications*, vol. 20, no. 8, pp. 5159–5170, 2021.

[42] Z. Zhang, Y. Xiao, Z. Ma, M. Xiao, Z. Ding, X. Lei, G. K. Karagiannidis, and P. Fan, "6g wireless networks: Vision, requirements, architecture, and key technologies," *IEEE Vehicular Technology Magazine*, vol. 14, no. 3, pp. 28–41, 2019.

[43] Q. Wu, M. Tao, D. W. K. Ng, W. Chen, and R. Schober, "Energy-efficient resource allocation for wireless powered communication networks," *IEEE Transactions on Wireless Communications*, vol. 15, no. 3, pp. 2312–2327, 2015.

[44] J. Wu, S. Rangan, and H. Zhang, *Green communications: theoretical fundamentals, algorithms, and applications*. CRC press, 2016.

[45] K. Gillingham, R. G. Newell, and K. Palmer, "Energy efficiency economics and policy," National bureau of economic research, Tech. Rep., 2009.

[46] H. Haci, H. Zhu, and J. Wang, "Performance of non-orthogonal multiple access with a novel asynchronous interference cancellation technique," *IEEE Transactions on Communications*, vol. 65, no. 3, pp. 1319–1335, 2017.

[47] B. Ling, C. Dong, J. Dai, and J. Lin, "Multiple decision aided successive interference cancellation receiver for noma systems," *IEEE Wireless Communications Letters*, vol. 6, no. 4, pp. 498–501, 2017.

[48] F. Jameel, M. Nabeel, and W. U. Khan, "Multi-tone carrier backscatter communications for massive iot networks," in *Wireless-Powered Backscatter Communications for Internet of Things*.  Springer, 2021, pp. 39–50.

[49] Z. Chi, Y. Li, H. Sun, Y. Yao, Z. Lu, and T. Zhu, "B2w2: N-way concurrent communication for iot devices," in *Proceedings of the 14th ACM Conference on Embedded Network Sensor Systems CD-ROM*, 2016, pp. 245–258.

[50] R. Long, Y.-C. Liang, Y. Pei, and E. G. Larsson, "Active-load assisted symbiotic radio system in cognitive radio network," in *2020 IEEE 21st International Workshop on Signal Processing Advances in Wireless Communications (SPAWC)*.  IEEE, 2020, pp. 1–5.

[51] B. R. Marks and G. P. Wright, "A general inner approximation algorithm for nonconvex mathematical programs," *Operations research*, vol. 26, no. 4, pp. 681–683, 1978.

[52] S. Boyd, L. Xiao, and A. Mutapcic, "Subgradient methods," *lecture notes of EE392o, Stanford University, Autumn Quarter*, vol. 2004, pp. 2004–2005, 2003.

[53] Z.-Q. Luo, W.-K. Ma, A. M.-C. So, Y. Ye, and S. Zhang, "Semidefinite relaxation of quadratic optimization problems," *IEEE Signal Processing Magazine*, vol. 27, no. 3, pp. 20–34, 2010.

[54] R. Horst and N. V. Thoai, "Dc programming: overview," *Journal of Optimization Theory and Applications*, vol. 103, no. 1, pp. 1–43, 1999.

[55] J. Nocedal, "Wright st. numerical optimization," 2006.

[56] J. F. Sturm, "Using sedumi 1.02, a matlab toolbox for optimization over symmetric cones," *Optimization methods and software*, vol. 11, no. 1-4, pp. 625–653, 1999.

[57] S. Boyd, S. P. Boyd, and L. Vandenberghe, *Convex optimization*.  Cambridge university press, 2004.

[58] A. Ben-Tal and A. Nemirovski, "On polyhedral approximations of the second-order cone," *Mathematics of Operations Research*, vol. 26, no. 2, pp. 193–205, 2001.

[59] Y. Ye, *Interior point algorithms: theory and analysis*.  John Wiley & Sons, 2011.

[60] A. Ben-Tal and A. Nemirovski, *Lectures on modern convex optimization: analysis, algorithms, and engineering applications*.  SIAM, 2001.

[61] B. Martinez, M. Monton, I. Vilajosana, and J. D. Prades, "The power of models: Modeling power consumption for iot devices," *IEEE Sensors Journal*, vol. 15, no. 10, pp. 5777–5789, 2015.

[62] M. S. Mahmoud and A. A. Mohamad, "A study of efficient power consumption wireless communication techniques/modules for internet of things (iot) applications," 2016.

[63] J. Finnegan and S. Brown, "An analysis of the energy consumption of lpwa-based iot devices," in *2018 International Symposium on Networks, Computers and Communications (ISNCC)*.  IEEE, 2018, pp. 1–6.

[64] D. Poluektov, M. Polovov, P. Kharin, M. Stusek, K. Zeman, P. Masek, I. Gudkova, J. Hosek, and K. Samouylov, "On the performance of lorawan in smart city: End-device design and communication coverage," in *International Conference on Distributed Computer and Communication Networks*.  Springer, 2019, pp. 15–29.

[65] S. K. Gharghan, R. Nordin, and M. Ismail, "Energy-efficient zigbee-based wireless sensor network for track bicycle performance monitoring," *Sensors*, vol. 14, no. 8, pp. 15 573–15 592, 2014.